ELSEVIER

Polymer 40 (1999) 3367–3382

polymer

Effects of bromine substitution on the physical and gas transport properties of five series of glassy polymers

M.S. McCaig, E.D. Seo, D.R. Paul*

Department of Chemical Engineering and Center for Polymer Research, University of Texas at Austin, Austin, TX 78712, USA

Received 8 June 1998; accepted 28 July 1998

Abstract

The effects of bromine substitution on the physical and gas transport properties were examined for five families of tetra-substituted glassy polymers: bisphenol A polycarbonates (PC), hexafluoro-polycarbonates (HFPC), hexafluorobisphenol-*tertiary* butyl isophthalates (HFBP-tBIA), fluorenebisphenol-*t*-butyl isophthalates (FBP-tBIA) and bisphenol A-*t*-butyl isophthalates (BPA-tBIA). Additionally, the thermal response of the substituted BPA-tBIA polymers was explored to elucidate the effects of bromine substitution on the activation energies of permeation and diffusion and on the heat of gas sorption. Compared to its methyl-substituted analog, each bromine-substituted polymer had a higher cohesive energy density, a higher glass transition temperature and a lower oxygen-specific fractional free volume. Bromine substitution significantly reduced O_2 and CO_2 permeability and substantially increased both O_2/N_2 and CO_2/CH_4 selectivity. An increase in the activation energy of diffusion for N_2 compared to O_2, and for CH_4 compared to CO_2, may be credited for the majority of the selectivity gain. A new method for evaluating penetrant-dependent fractional free volume proved to be a valuable tool in determining the effects of structural changes on gas transport behavior.

Keywords: Bromine substitution; Physical properties; Gas transport properties

1. Introduction

Polymeric materials with high permeability and high selectivity are essential to the competitive advantage of membrane-based gas separation processes. The foundation for developing new materials of this type requires a thorough understanding of the structure–property relationships established from studies involving a wide range of polymers. From this knowledge, other materials may be developed that exploit the unique attributes of various structural moieties. The tradeoff between permeability and selectivity observed in polymeric membranes led Robeson [1] to propose an 'upper bound' on a plot of selectivity versus permeability above which no polymers are currently known to exist.

Polymers made from bisphenol monomers with bromine substitution on the aromatic rings *ortho* to the hydroxyl groups have been shown to exhibit increased O_2/N_2 selectivity without substantial loss in oxygen permeability relative to their structural analogs containing no bromine atoms [2–4]. Two possible explanations of this behavior have been proposed. The first suggests that the bromine atoms contribute to steric hindrance of torsional rotations about the phenyl ring [2]; hindrance of such rotation has long been associated with increased permselectivity [5]. The second proposal involves polymer/penetrant interactions; i.e., the bromine atoms lead to a polar structure that preferably interacts with one of these gases so that the O_2/N_2 solubility selectivity is increased [6]. These two ideas are not necessarily mutually exclusive.

This paper explores the effects of bromine substitution on the gas transport behavior and other physical properties of glassy polymers. The glass transition temperature, fractional free volume, permeability, diffusivity and solubility of a number of bisphenol-based polymers are examined as a function of the degree of bromine substitution. The effects of bromine substitution on the activation energy of diffusion and the heat of sorption were determined to further assess the observed changes in O_2/N_2 and CO_2/CH_4 selectivity.

2. Strategy

This paper examines the effects of bromine substitution on the physical and gas transport properties of five families of tetra-substituted polymers; in each polymer, the positions

* Corresponding author.

0032-3861/99/$ - see front matter
PII: S0032-3861(98)00570-9

Table 1
Polymer structures and physical properties

Structure[a]				Polymer abbreviation	T_g (°C)	Density (g cm^{-3})	FFV[b]
R_1	R_2	R_3	R_4				
CH_3	CH_3	$-C(CH_3)_2-$	c	TMPC[d]	193	1.083	0.180
Br	Br	$-C(CH_3)_2-$	c	TBPC[d]	263	1.953	0.178
CH_3	CH_3	$-C(CF_3)_2-$	c	TMHFPC[e]	208	1.286	0.217
Br	Br	$-C(CF_3)_2-$	c	TBHFPC[e]	255	1.987	0.239
CH_3	CH_3	$-C(CF_3)_2-$	f	TMHFBP-tBIA[g]	242	1.189	0.216
Br	Br	$-C(CF_3)_2-$	f	TBHFBP-tBIA[h]	261	1.694	0.219
CH_3	CH_3	$-C(CH_3)_2-$	f	TMBPA-tBIA[i]	231	1.055	0.189
Br	CH_3	$-C(CH_3)_2-$	f	DMDBBPA-tBIA[i]	252	1.334	0.190
Br	Br	$-C(CH_3)_2-$	f	TBBPA-tBIA[i]	261	1.595	0.199
CH_3	CH_3	j	f	TMFBP-tBIA[i]	311	1.078	0.207
Br	CH_3	j	f	DMDBFBP-tBIA[i]	316	1.303	0.209
Br	Br	j	f	TBFBP-tBIA[h]	327	1.525	0.211

[a] The general polymer structure is as follows:

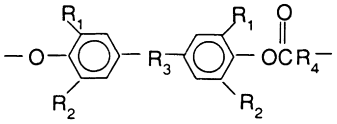

[b] FFV calculated by Bondi method [8].
[c] There is no R_4 for the polycarbonates.
[d] Data from Muraganandam et al. [3].
[e] Data from Hellums et al. [2].

f

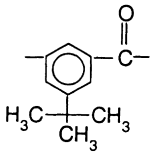

[g] Data from Ruiz-Trevino and Paul [7].
[h] Data from Pixton and Paul [4].
[i] Data obtained in this study.
j

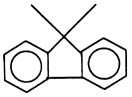

ortho to the hydroxyl groups of the bisphenol monomer are occupied by either methyl groups, bromine atoms or a combination of these groups. The families investigated, each designated by the unsubstituted analog, are: bisphenol A polycarbonates (PC) [3], hexafluoropolycarbonates (HFPC) [2], hexafluorobisphenol-*tertiary* butyl isophthalates (HFBP-tBIA) [4,7], fluorenebisphenol-*t*-butyl isophthalates (FBP-tBIA) [4] and bisphenol A-*t*-butyl isophthalates (BPA-tBIA). Structures, acronyms and sources for the polymers are given in Table 1. Comparing tetra-substituted polymers with varying degrees of methyl and bromine substitution minimizes the effects of simple steric hindrance because of the similarity in size of methyl groups and bromine atoms. This allows isolation of the specific effects of bromine substitution since simple steric hindrance of rotation of the substituted phenyl ring should be approximately the same regardless of which of the two substituents is present. Where possible, a dimethyl-dibromo substituted polymer has been used to represent an intermediate structure between tetramethyl and tetrabromo substitution. A simple comparison between tetrabromo substituted polymers and the analogous structure where hydrogens occupy the *ortho* positions would involve two effects; the simple size-related steric effect and any specific effect of the bromine substituent.

Gas transport and other physical properties of the tetramethyl and tetrabromo members of the PC, HFPC and HFBP-tBIA families mentioned above have already been reported in the literature. In addition to the data reported in the literature [4] for TBFBP-tBIA, the synthesis and characterization reported here for the two new polymers, TMFBP-tBIA and DMDBFBP-tBIA, completes the data for the FBP-tBIA family of polymers. Gas transport data for the three substituted BPA-tBIA polymers were collected over a range of temperatures to examine the effects of bromine substitution on the activation energy of diffusion and the heat of gas sorption within this series. This required the synthesis and characterization of a new polymer (DMDBBPA-tBIA) and the synthesis and recharacterization of two previously studied polymers (TMBPA-tBIA [9] and TBBPA-tBIA [4]). Thus, experimental data for three new polymers are presented for the first time in this paper.

3. Experimental section

Information about the monomers used here to synthesize the BPA-tBIA and FBP-tBIA series of polymers is given in Table 2. Tetramethyl-fluorenebisphenol (TMFBP) was prepared by condensing 9-fluorenenone and 2,6-dimethyl phenol in the presence of hydrogen chloride [10,11]. Dimethyl-dibromo-fluorenebisphenol (DMDBFBP) and dimethyl-dibromobisphenol A (DMDBBPA) were both prepared by direct bromination of the dimethyl precursor

[4]. 5-*t*-Butyl isophthaloyl dichloride (tBIA) was synthesized by refluxing the dicarboxylic acid with excess thionyl chloride, and purified by vacuum distillation [5]. The polymer structures and their physical characteristics are listed in Table 1. The five polymers synthesized for this study were: TMBPA-tBIA, DMDBBPA-tBIA, TBBPA-tBIA, TMFBP-tBIA and DMDBFBP-tBIA. All were made by an interfacial polymerization method described by Morgan [11]. The polymers were reprecipitated twice from chloroform into ethanol and then vacuum dried to remove residual solvent.

The glass transition temperature (T_g) of each polymer was measured using a Perkin–Elmer DSC-7 differential scanning calorimeter at a heating rate of 20°C min^{-1}. The polymer samples were heated twice and the T_g was evaluated as the onset of the transition on the second scan. All five polymers appear to be amorphous, due to their clarity and the absence of a crystalline melting point. The density of each polymer was measured in a density gradient column based on either aqueous calcium nitrate solutions or aqueous zinc chloride solutions at 30°C.

Polymer films (1–2.8 mil) were cast from chloroform (2.5% wt) onto glass plates in a glove bag. The films were then vacuum dried at room temperature for 24 h and then at 150°C for five days. Thermogravimetric analysis (TGA) using a Perkin–Elmer TGA-7 was used to confirm the complete removal of solvent.

Pure gas permeability coefficients were evaluated at temperatures ranging from 35 to 57°C for O_2, N_2, CO_2 and CH_4, using a standard pressure-rise type permeation cell and following standard procedures employed in this laboratory [9]. The gas permeability coefficients (P) were measured at an upstream driving pressure of 2 atm for O_2 and N_2 and 10 atm for CO_2 and CH_4. The average diffusion coefficients (D) were calculated from experimentally measured time lags, using

$$D = \frac{l^2}{6\theta} \tag{1}$$

where l is the film thickness and θ is the diffusion time lag. The apparent solubility coefficients (S) were estimated from the permeability and diffusion coefficients by the relation

$$P = DS \tag{2}$$

4. Experimental results

Three new polymers, DMDBBPA-tBIA, TMFBP-tBIA and DMDBFBP-tBIA, were synthesized and their permeation properties were measured for the first time; these polymers complete the substituted BPA-tBIA and FBP-tBIA families of polymers. In addition, TMBPA-tBIA and TBBPA-tBIA were also synthesized and recharacterized. The gas transport properties of all five polymers were measured at 35°C and 2 atm for O_2 and N_2 and at 35°C and 10 atm for CO_2 and CH_4; the results are shown in Table 3. Fig. 1(a) and (b) illustrate the position of these polymers with respect to the Robeson 'upper bound' for the O_2/N_2 and the CO_2/CH_4 permselectivity tradeoff; the open symbols represent the new polymers and the closed symbols represent the retested polymers. The methyl-substituted polymers display higher permeability and lower selectivity for both gas pairs when compared to their bromine-substituted analogs. As bromine substitution is increased, the tradeoff shifts to lower permeability and higher selectivity, approaching the upper bound for both O_2/N_2 and CO_2/CH_4 separation. The effect of bromine substitution on the O_2/N_2 and CO_2/CH_4 permselectivity performance for all five polymer families mentioned in the strategy section will be examined in a subsequent section.

It was felt that measurement of the activation energy of diffusion (E_D) and the heat of gas sorption (H_S) for at least one of the substituted families would add additional insight into why bromine substitution causes these changes. Thus, permeability coefficients and time-lag diffusion coefficients were measured at 2 atm for O_2 and N_2 for temperatures ranging from 35 to 50°C, and at 10 atm for CO_2 and CH_4 for temperatures ranging from 35 to 57°C, for TMBPA-tBIA, DMDBBPA-tBIA and TBBPA-tBIA; duplicate measurements were performed at each temperature. The gas transport data at 35°C were available in the literature for TMBPA-tBIA and TBBPA-tBIA, but these values were retested to maintain experimental consistency with the values obtained at higher temperatures. Figs. 2–5 show the results for O_2, N_2, CO_2 and CH_4 in the form of Arrhenius relations, i.e.

$$P = P_0 e^{-E_P/RT} \tag{3}$$

$$D = D_0 e^{-E_D/RT} \tag{4}$$

Table 2
Monomer sources and purification

Monomer	Source	Purification	Melting point[a] (°C)
tetramethyl-bisphenol A (TMBPA)	Ken Seika	none	165–167
dimethyldibromo-bisphenol A (DMBDBBPA)	synthesis	sublimation	120–121
tetrabromo-bisphenol A (TBBPA)	Lancaster	sublimation	180–182
tetramethyl-fluorenebisphenol (TMFBP)	synthesis	recrystallization	263–264
dimethyldibromo-fluorenebisphenol (DMDBFBP)	synthesis	recrystallization	240–242
5-*t*-butyl isophthaloyl dichloride (tBIA)	synthesis	distillation	43–44

[a]After purification.

Table 3
Mobility and solubility components of the O_2/N_2[a] and CO_2/CH_4[b] separation factor

Polymer	P_{O_2} (barrer)[c]	α_{O_2/N_2}	D_{O_2}[d] (10^{-8}[cm^2 s^{-1}])	D_{O_2}/D_{N_2}	S_{O_2}[e] $\left[\frac{cm^3(STP)}{cm^3\ atm}\right]$	S_{O_2}/S_{N_2}
TMBPA-tBIA	13.1	4.89	14.5	3.51	0.69	1.39
DMDBBPA-tBIA	6.27	5.92	7.53	4.30	0.63	1.38
TBBPA-tBIA	5.40	6.35	5.85	4.50	0.70	1.40
TMFBP-tBIA	28.1	4.68				
DMDBFBP-tBIA	17.9	5.54				
Polymer	P_{CO_2}	α_{CO_2/CH_4}	D_{CO_2}	D_{CO_2}/D_{CH_4}	S_{CO_2}	S_{CO_2}/S_{CH_4}
TMBPA-tBIA	46.0	16.1	7.93	5.43	4.42	2.98
DMDBBPA-tBIA	22.7	21.5	4.58	7.76	3.77	2.77
TBBPA-tBIA	19.7	23.5	3.23	7.43	4.65	3.16
TMFBP-tBIA	110	16.8				
DMDBFBP-tBIA	71.0	21.5				

[a]Data at 35°C and 2 atm.
[b]Data at 35°C and 10 atm.
[c]1 barrer $= 10^{-10}\left[\frac{cm^3\ (STP)\ cm}{cm^2\ s\ cm\ Hg}\right]$.
[d]From time-lag method (Eq. (1)).
[e]Estimated from $S = P/D$.

where R is the universal gas constant. The data fit these relations accurately and follow the expected trends of increasing permeability and diffusivity as temperature increases. The activation energies of permeation (E_P) and diffusion (E_D) determined from these plots and the calculated heats of sorption (H_S), i.e. $H_S = E_P - E_D$, along with the appropriate pre-exponential factors, $S_O = P_O/D_O$ for the three substituted BPA-tBIA polymers, are listed in Table 4. The effect of bromine substitution on the activation energies of permeation (E_P) and diffusion (E_D) and heats of sorption (H_S) will be examined in a subsequent section.

5. Bromine substitution effects for polyesters and polycarbonates

5.1. Physical property trends

Cohesive energy density (CED) provides a measure of the attractive intermolecular forces between polymer chains. Values for the CED of the members of four of the five polymer families of interest here were estimated by the group contribution method described by van Krevelen [12]; the effect of bromine substitution on these polymers is illustrated in Fig. 6(a). The absence of a fluorene connector group in the van Krevelen database precludes CED estimates for fluorene bisphenol polymers by this technique; therefore, the FBP-tBIA series is not included in Fig. 6(a), but a similar trend would be evident. For all four polymer families, the CED increases significantly as bromine substitution increases.

In all cases, the glass transition temperature of each of the bromine-substituted polymers is higher than that of its methyl-substituted analog. Fig. 6(b) shows the increase in T_g associated with increased bromine substitution. Furthermore, the magnitude of the T_g increase is dependent on the polymer structure; the two polycarbonate families show the greatest increase in T_g while the three polyarylate families have a smaller, but still significant, increase in T_g associated with bromine substitution.

The diffusion of penetrants in polymers is often interpreted in terms of the free volume of the polymer; similarly, free volume is also a factor in the solubility of gases in polymers [13]. Thus, gas permeability coefficients have been correlated to polymer free volume with considerable success. Fractional free volume (FFV) is frequently estimated from the experimental density and a calculated occupied volume, V_o, using the following definition [8,12]

$$FFV = (V - V_o)/V \tag{5}$$

where V is the measured polymer specific volume; the occupied volume can be estimated from the van der Waals volumes, $(V_w)_k$, of the various structural groups according to the relation

$$V_o = 1.3 \sum_{k=1}^{K} (V_w)_k \tag{6}$$

This method yields a value of the FFV that is characteristic of the polymer and independent of the penetrating gas. The trend in FFV associated with replacing methyl substituents ($V_w = 13.67\ cm^3\ mol^{-1}$) with bromine atoms ($V_w = 14.6\ cm^3\ mol^{-1}$) is seen in Fig. 7(a). The FFV estimated in this way increases for the HFPC-, HFBP-tBIA-, FBP-tBIA- and BPA-tBIA-based polymers as bromine

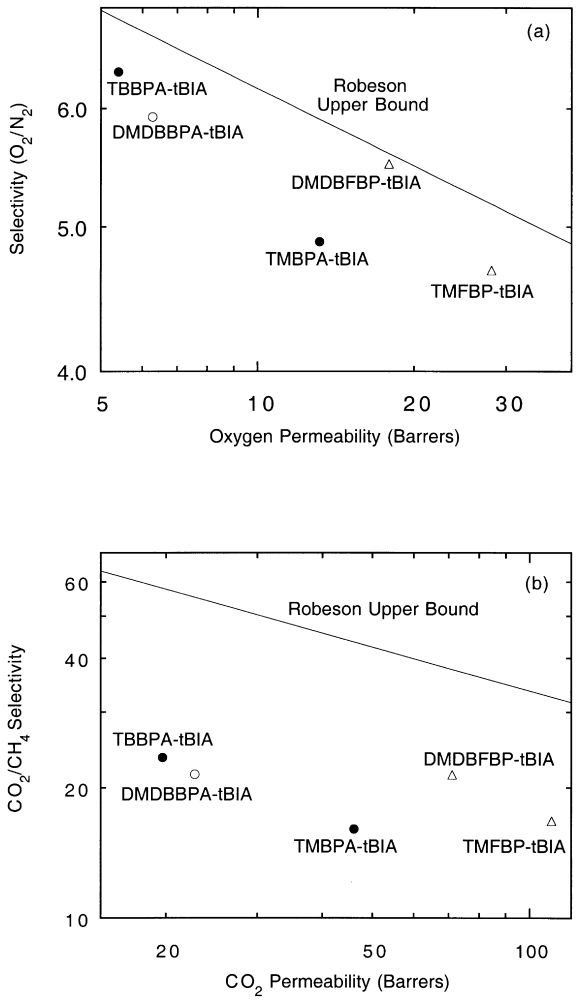

Fig. 1. Effect of methyl and bromine substitution on (a) oxygen permeability and oxygen/nitrogen selectivity at 2 atm and 35°C and (b) carbon dioxide permeability and carbon dioxide/methane selectivity at 10 atm and 35°C for the five polymers synthesized for this study. The open symbols (○, △) represent new polymers and the solid symbols (●) represent polymers that have been retested. The solid line on both plots depicts the 'upper bound' proposed by Robeson [1].

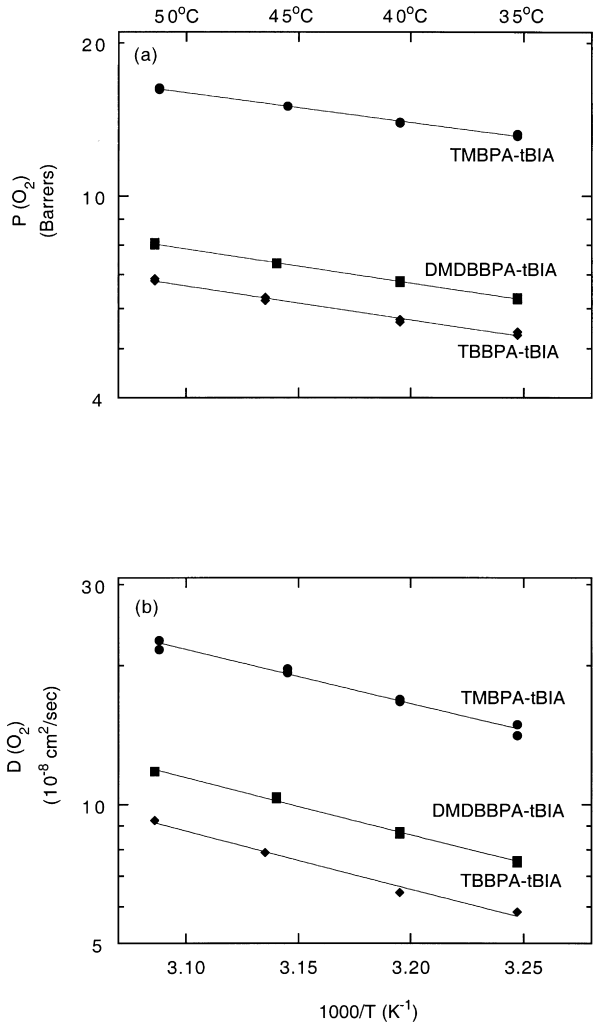

Fig. 2. Temperature dependence of (a) oxygen permeability coefficients and (b) oxygen diffusion coefficients for the BPA-tBIA polymer series at 2 atm. Duplicate measurements are shown at each temperature.

substitution increases, and decreases slightly for the PC-based polymers. No explanation for these conflicting trends is immediately obvious.

The polymer free volume available for penetrant transport may depend on the size or character of the penetrant. Park and Paul [13] proposed a new scheme for predicting gas permeability coefficients for glassy polymers in terms of the free volume framework by redefining the occupied volume in a way that accounts for any effect of the nature of the penetrant molecule. This group contribution scheme replaces Eqs. (5) and (6) with the following

$$\mathrm{FFV}_n = [V - (V_o)_n]/V \tag{7}$$

$$(V_o)_n = \sum_{k=1}^{K} \gamma_{nk}(V_w)_k \tag{8}$$

where γ_{nk} is a constant unique to each structural unit k and gas type n; values for γ_{nk} were evaluated by Park and Paul from permeability data for a large number of glassy polymers. The fractional free volume computed for oxygen (FFV_{O_2}) is shown in Fig. 7(b) as a function of the extent of bromine substitution. In every case, FFV_{O_2} decreases as bromine substitution increases. Although not shown, FFV_{N_2} shows similar trends. The similarity in trends across all the polymer families indicates that the penetrant-specific fractional free volume estimated from Eqs. (7) and (8) may be more informative than the general fractional free volume when comparing structural changes, since consideration of any polymer–penetrant interactions is included.

The physical properties of the polymers studied were affected to varying degrees by replacement of methyl groups with bromine atoms. The cohesive energy density increased significantly, and the glass transition temperature increased to a lesser extent; these trends are indicative of a higher degree of chain attraction and chain rigidity in the

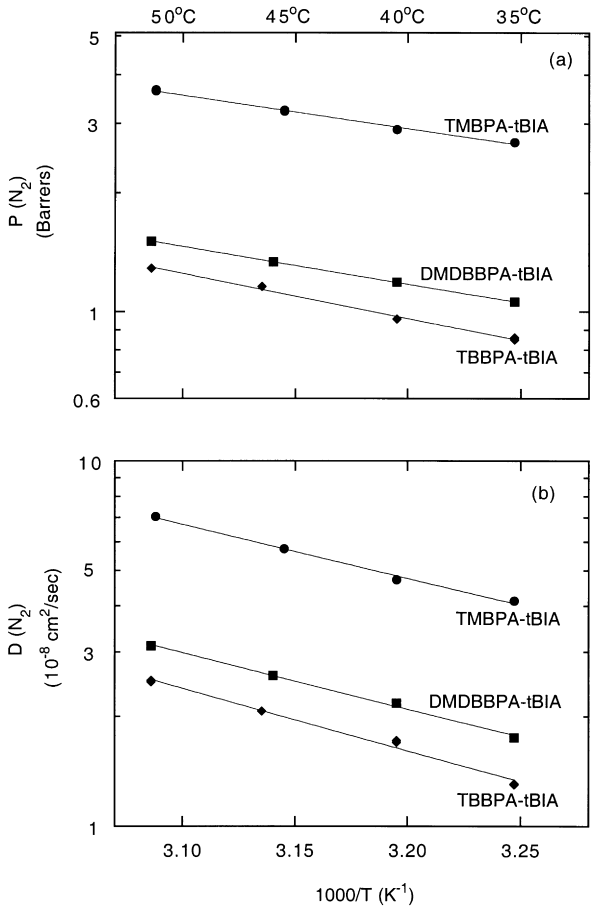

Fig. 3. Temperature dependence of (a) nitrogen permeability coefficients and (b) nitrogen diffusion coefficients for the substituted BPA-tBIA polymer series at 2 atm.

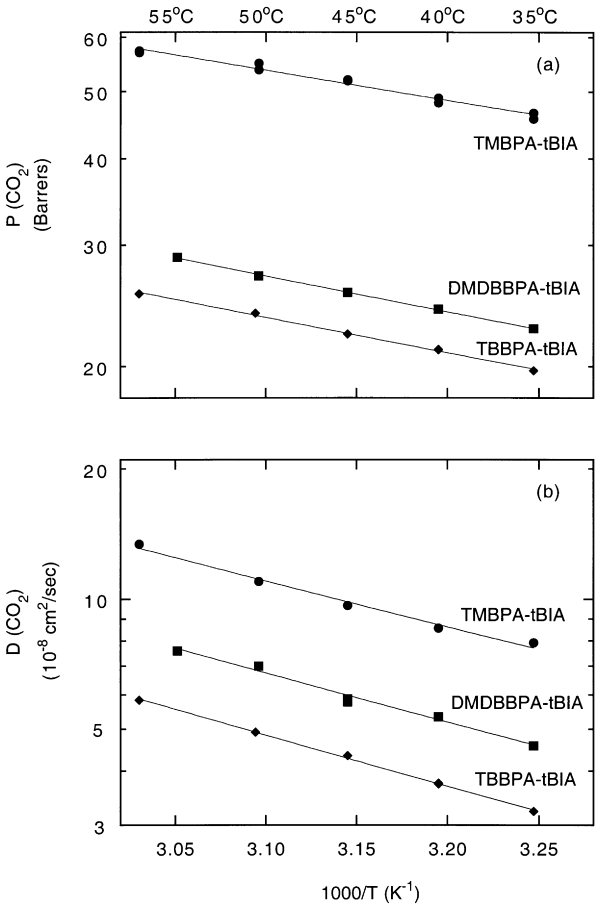

Fig. 4. Temperature dependence of (a) carbon dioxide permeability coefficients and (b) carbon dioxide diffusion coefficients for the substituted BPA-tBIA polymer series at 10 atm.

bromine-substituted polymers. The increase in chain attraction is also reflected as a substantial loss in the FFV_{O_2} as bromine substitution increases, even though the bromine atoms ($V_w = 14.6\ cm^3\ mol^{-1}$) are slightly larger than the methyl groups ($V_w = 13.67\ cm^3\ mol^{-1}$). The Park and Paul method of estimating penetrant-dependent FFV was of great value in investigating structural changes due to its consideration of polymer–penetrant interactions.

5.2. Gas transport property trends

Pure gas permeability, diffusivity and solubility coefficients for O_2 and CO_2 as well as O_2/N_2 and CO_2/CH_4 ideal separation factors for the various polymers considered here are summarized in Table 5 and Table 6. Two sets of data for TMBPA-tBIA and TBBPA-tBIA are included; the values in parentheses were taken from previously reported studies whereas the values without parentheses were measured as part of this work. The differences in the two data sets are not significant for the permeability coefficients but some substantial differences in diffusivity and solubility coefficients may be noted, which can be attributed, in part, to using different methods to obtain the data, as will be discussed subsequently. Ideal permselectivities ($\alpha_{A/B}$) were calculated from

$$\alpha_{A/B} = P_A/P_B \quad (9)$$

where P_A and P_B are the permeability coefficients for pure gas A and pure gas B, respectively. Ideal permselectivity should provide a good estimate of actual mixed gas performance because of the relative lack of interaction between oxygen and nitrogen with the polymer; however, this may not be so at high pressures for CO_2/CH_4 because of the high solubility of CO_2. In all cases, going from tetra-methyl substitution to tetra-bromo substitution leads to a reduction in O_2 and CO_2 permeability, but a gain in O_2/N_2 and CO_2/CH_4 ideal selectivity.

Comparing the permselectivity performance of polymers is important for evaluating the effects of structural changes. The effect of methyl and bromine substitution on the relationship between oxygen permeability and O_2/N_2 selectivity for four of the polymer families of interest is shown in Fig. 8(a); the PC family is not represented because the

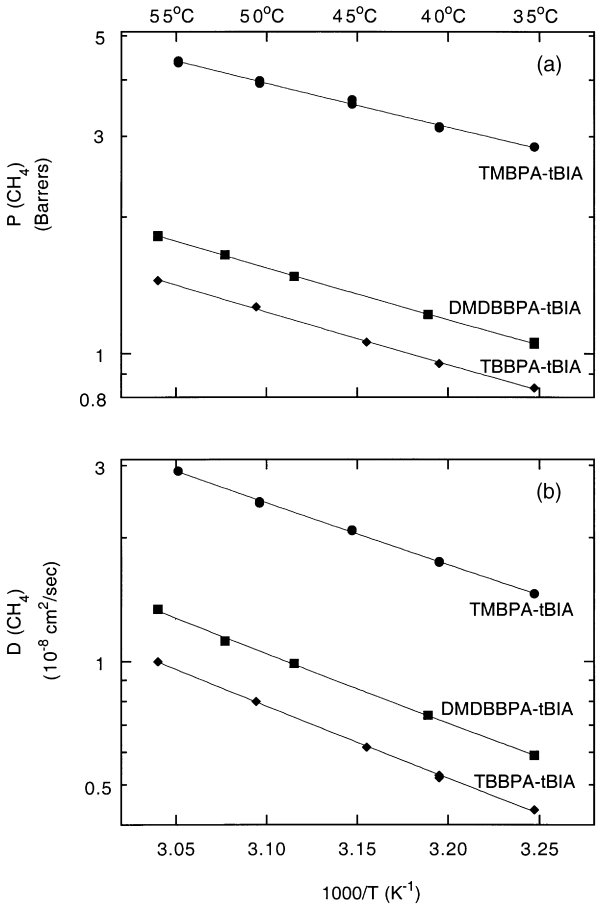

Fig. 5. Temperature dependence of (a) methane permeability coefficients and (b) methane diffusion coefficients for the substituted BPA-tBIA polymer series at 10 atm.

polymers are very far from the 'upper bound'. Tetra-methyl-substituted polymers have comparatively high oxygen permeability and low O_2/N_2 selectivity; this trade-off seems to be improved by bromine substitution to give a lower oxygen permeability but much higher O_2/N_2 selectivity. Bromine substitution leads to polymers that lie closer to the Robeson 'upper bound' curve with the exception of the HFPC family, which moves approximately parallel to the curve. Fig. 8(b) gives a similar comparison for the CO_2/CH_4 gas pair. Comparatively, the tetra-methyl-substituted polymers lie farther from the CO_2/CH_4 'upper bound' curve than is the case for O_2/N_2. Bromine substitution substantially improves the trade-off for the HFBP-tBIA and FBP-tBIA families, shifting them toward the 'upper bound' curve, whereas the BPA-tBIA moves slightly toward the curve and the HFPC family moves away from the curve.

As seen in Fig. 9(a) and (b), oxygen permeability decreases and O_2/N_2 selectivity increases as the degree of bromine substitution increases for each polymer family. In two cases (BPA-tBIA and FBP-tBIA), data are available to show the effect of replacing only two of the methyl units with bromine atoms. It appears that the majority of the reduction in O_2 permeability occurs upon di-substitution with bromine. The largest increase in O_2/N_2 selectivity resulting from bromine substitution is seen for the polycarbonates; however, the increases for the other polymers are also significant. Similar trends for the CO_2/CH_4 gas pair can be seen in Fig. 10(a) and (b): a decrease in CO_2 permeability and an increase in CO_2/CH_4 selectivity as bromine substitution increases. As with O_2 permeability, the dimethyl-dibromo substitution in the BPA-tBIA and FBP-tBIA families accounts for the majority of the CO_2 permeability

Table 4
Arrhenius and van't Hoff parameters for O_2, N_2, CO_2 and CH_4 transport in BPA-tBIA polymers

Polymers	E_P^a	P_o (barrer)	E_D^a	D_o (10^{-4}[cm^2 s^{-1}])	H_S^a	S_o $\left(10^{-3}\left[\frac{\text{cm}^3\ (\text{STP})}{\text{cm}^3\ \text{atm}}\right]\right)$
O_2:						
TMBPA-tBIA	2.68	1036	5.37	9.43	−2.69	8.35
DMDBBPA-tBIA	3.07	946	5.63	7.46	−2.56	9.64
TBBPA-tBIA	3.06	785	5.76	7.09	−2.70	8.41
N_2:						
TMBPA-tBIA	3.84	1466	6.79	26.8	−2.95	4.15
DMDBBPA-tBIA	4.36	1322	7.04	17.5	−2.68	5.74
TBBPA-tBIA	5.24	4454	7.84	49.0	−2.56	6.91
CO_2:						
TMBPA-tBIA	2.01	1230	4.87	2.21	−2.86	42.3
DMDBBPA-tBIA	2.37	1083	5.19	2.23	−2.83	36.9
TBBPA-tBIA	2.36	939	5.40	2.22	−3.04	32.1
CH_4:						
TMBPA-tBIA	4.41	3831	6.94	12.3	−2.53	26.9
DMDBBPA-tBIA	5.24	5455	7.75	18.5	−2.51	22.8
TBBPA-tBIA	5.33	5091	8.07	22.9	−2.74	16.9

[a]Units of E_P, E_D and H_S are kcal mol^{-1}.

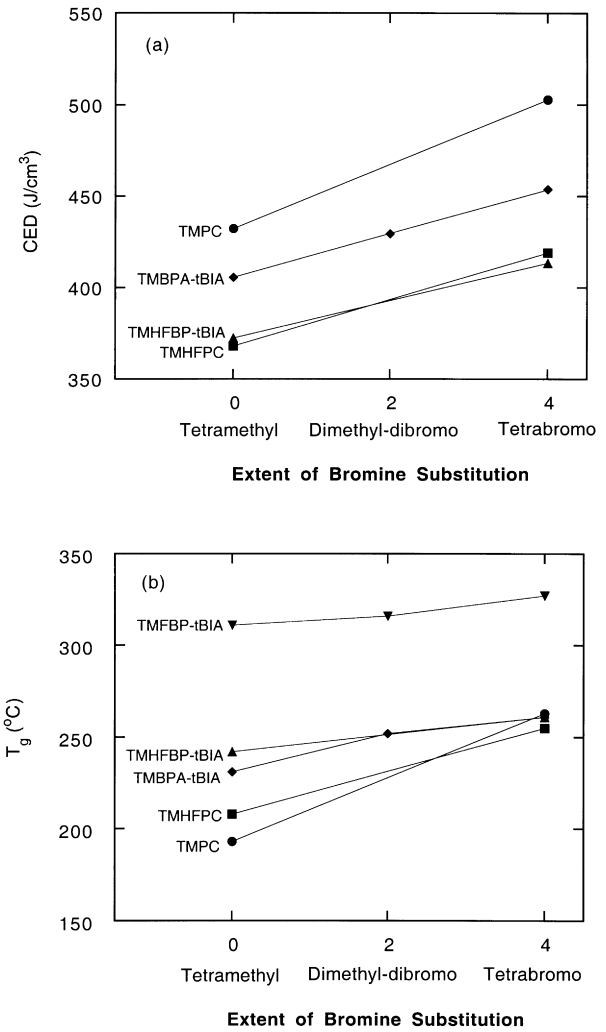

Fig. 6. Effect of replacing methyl groups with bromine atoms on (a) cohesive energy density and (b) glass transition temperature for the families of substituted polymers studied: PC [3] (●), HFPC [2] (■), HFBP-tBIA [4,7] (▲), FBP-tBIA [4] (▼) and BPA-tBIA (♦). The FBP-tBIA family is not included in the CED plot due to the absence of a fluorene group in the van Krevelen [12] database.

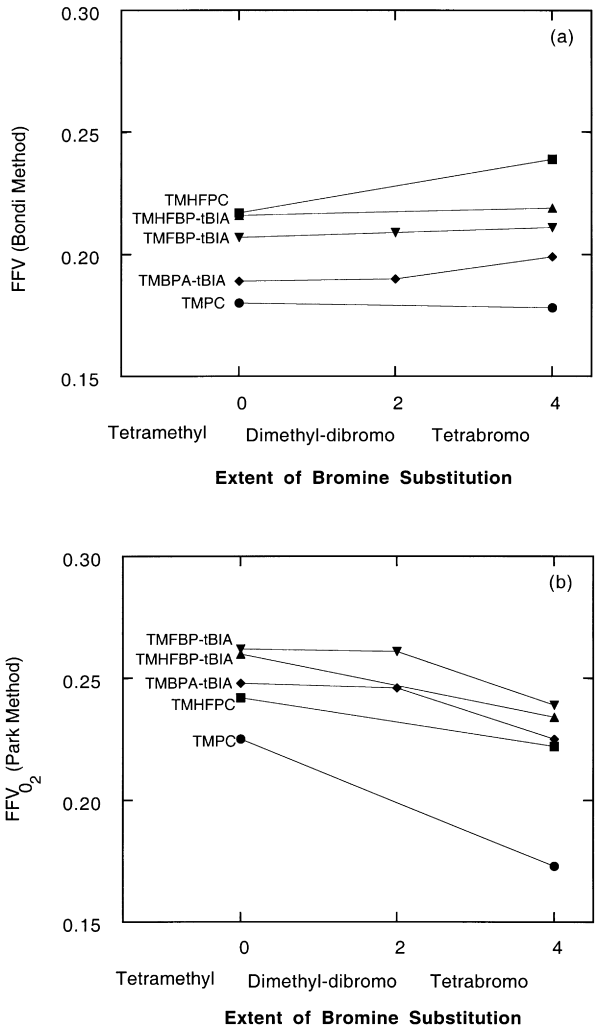

Fig. 7. Effect of replacing methyl groups with bromine atoms on (a) the fractional free volume computed by the Bondi method [8] and (b) the oxygen specific fractional free volume computed by the Park method [13] for the families of substituted polymers studied: PC [3] (●), HFPC [2] (■), HFBP-tBIA [4,7] (▲), FBP-tBIA [4] (▼) and BPA-tBIA (♦).

decrease in going from methyl groups to bromine atoms in the four *ortho* positions. The CO_2/CH_4 selectivity increase resulting from bromine substitution is significant for all the families; the PC and HFPC families show the largest increases.

The apparent diffusion coefficients reported in Tables 5 and 6 were determined by one of two methods. In one, the diffusion coefficients were calculated from experimentally measured time lags using Eq. (1). In the other, the diffusion coefficients were estimated from the experimentally determined permeability and solubility coefficients using Eq. (2). Diffusion coefficients are compared in Fig. 11(a) and (b) to establish trends; caution should be exercised because time-lag calculated diffusion coefficients may be different than those estimated from permeability and sorption. The effects of bromine substitution on the apparent O_2 diffusivity and O_2/N_2 diffusivity selectivity are similar to those seen for permeability. The O_2 diffusivity decreases and the O_2/N_2 diffusivity selectivity increases for all polymers as bromine substitution increases. Results for FBP-tBIA polymers are not shown because the data are incomplete at this time. It is evident from Fig. 12(a) that CO_2 diffusivity decreases as bromine substitution increases; the HFPC family shows the greatest decline in CO_2 diffusivity. Each family of polymers shows a similar increase in CO_2/CH_4 diffusivity selectivity, as seen in Fig. 12(b). The majority of the diffusivity selectivity increase occurs upon di-substitution with bromine in the BPA-tBIA family.

Solubility coefficients were also determined utilizing one of two methods. In one, solubility coefficients were calculated from the secant slope of experimental sorption isotherms. In the other, experimental permeability and diffusivity (by time lag) coefficients were used to estimate solubility coefficients from Eq. (2). Fig. 13(a) shows the small increase in O_2 solubility associated with bromine

Table 5
Mobility and solubility components of the O_2/N_2 separation factor[a]

Polymer	P_{O_2} [c] (barrer)	α_{O_2/N_2}	D_{O_2} [d] (10^{-8}[cm^2 s^{-1}])	D_{O_2}/D_{N_2}	S_{O_2} [e] $\left[\frac{\text{cm}^3\ (\text{STP})}{\text{cm}^3\ \text{atm}}\right]$	S_{O_2}/S_{N_2}
TMPC[b]	5.59	5.13	8.1[c]	3.77	0.52[d]	1.45
TBPC[b]	1.36	6.36	1.69[c]	4.97	0.61[d]	1.49
TMHFPC[e]	32.0	4.16	31.0[d]	3.2	0.78[f]	1.3
TBHFPC[e]	9.7	5.4	9.2[d]	4.2	0.80[f]	1.3
TMHFBP-tBIA[g]	40.0	4.3	36.9[c]	3.1	0.83[d]	1.39
TBHFBP-tBIA[h]	22.1	4.94	18.1[d]	4.38	0.93[f]	1.13
TMBPA-tBIA	13.1	4.89	14.5[c]	3.51	0.69[d]	1.39
(TMBPA-tBIA[i])	(12.2)	(4.84)	(12.5[d])	(3.82)	(0.74[f])	(1.26)
DMDBBPA-tBIA	6.27	5.92	7.53[c]	4.30	0.63[d]	1.38
TBBPA-tBIA	5.40	6.35	5.85[c]	4.46	0.70[d]	1.40
(TBBPA-tBIA[h])	(5.63)	(6.25)	(6.98[d])	(3.62)	(0.62[f])	(1.73)
TMFBP-tBIA	28.1	4.68				
DMDBFBP-tBIA	15.4	5.54				
TBFBP-tBIA[h]	16.8	5.71	12.7[d]	4.03	1.01[f]	1.42

[a]Data at 35°C and 2 atm.
[b]Data from Muraganandam et al. [3].
[c]Determined by time-lag method (Eq. (1)).
[d]Estimated by $P = DS$.
[e]Data from Hellums et al. [2].
[f]Determined by sorption.
[g]Data from Ruiz-Trevino and Paul [7].
[h]Data from Pixton and Paul [4].
[i]Data from Pixton and Paul [9].

Table 6
Mobility and solubility components of the CO_2/CH_4 separation factor[a]

Polymer	P_{CO_2} (barrer)	α_{CO_2/CH_4}	D_{CO_2} (10^{-8}[cm^2 s^{-1}])	D_{CO_2}/D_{CH_4}	S_{CO_2} $\left[\frac{\text{cm}^2\ (\text{STP})}{\text{cm}^3\ \text{atm}}\right]$	S_{CO_2}/S_{CH_4}
TMPC[b]	17.6	22	6.11[c]	7.54	2.18[d]	2.92
TBPC[b]	4.23	33.6	1.66[c]	12.8	1.93[d]	2.63
TMHFPC[e]	110	24	21.0[c]	7.0	4.1[d]	3.4
TBHFPC[e]	32	36	6.4[c]	11.7	3.9[d]	3.1
TMHFBP-tBIA[f]	140	18	19.2[g]	5.5	5.5[d]	3.2
TBHFBP-tBIA[h]	85.1	25.3	16.3[d]	9.31	3.98[f]	2.72
TMBPA-tBIA	46.0	16.1	7.93[c]	5.43	4.42[d]	2.98
(TMBPA-tBIA[i])	(44.6)	(17.4)	(11.2[d])	(6.19)	(3.04[f])	(2.8)
DMDBBPA-tBIA	22.7	21.5	4.58[c]	7.76	3.77[d]	2.77
TBBPA-tBIA	19.7	23.5	3.23[c]	7.43	4.65[d]	3.16
(TBBPA-tBIA[h])	(21.5)	(25.2)	(4.98[d])	(9.21)	(3.28[f])	(2.73)
TMFBP-tBIA	110	16.8				
DMDBFBP-tBIA	71	21.5				
TBFBP-tBIA[h]	69.5	25.1	11.9[d]	9.68	4.42[f]	2.59

[a]Data at 35°C and 10 atm.
[b]Data from Muraganandam et al. [3].
[c]Estimated by $P = DS$.
[d]Determined by sorption.
[e]Data from Hellums et al. [2].
[f]Data from Ruiz-Trevino and Paul [7].
[g]Determined by time-lag method (Eq. (1)).
[h]Data from Pixton and Paul [4].
[i]Data from Pixton and Paul [9].

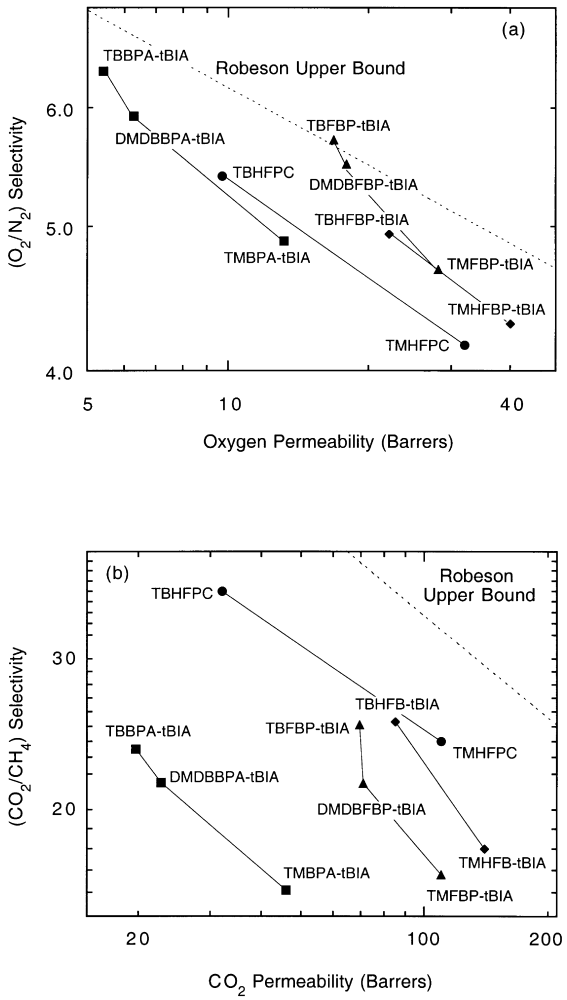

Fig. 8. Effect of methyl and bromine substitution on (a) oxygen permeability and oxygen/nitrogen selectivity at 2 atm and 35°C and (b) carbon dioxide permeability and carbon dioxide/methane selectivity at 10 atm and 35°C for four of the families of substituted polymers studied: HFPC [2] (■), HFBP-tBIA [4,7] (▲), FBP-tBIA [4] (▼) and BPA-tBIA (◆). The PC family of polymers is not shown because of its distance from both Robeson 'upper bound' curves which are illustrated by the dashed line on each figure.

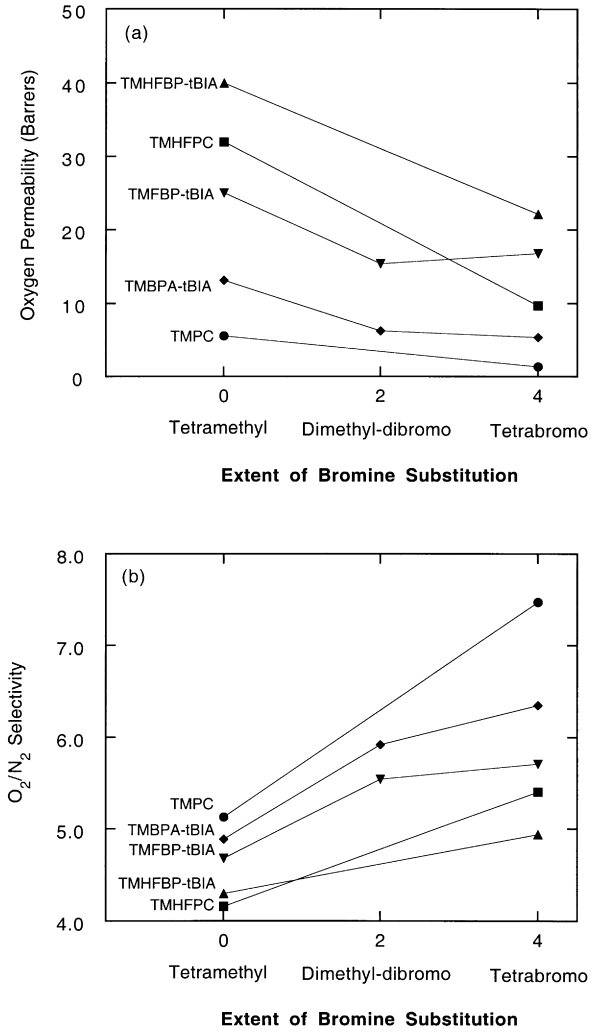

Fig. 9. Effect of replacing methyl groups with bromine atoms on (a) oxygen permeability coefficients and (b) oxygen/nitrogen selectivity at 2 atm and 35°C for the families of substituted polymers studied: PC [3] (●), HFPC [2] (■), HFBP-tBIA [4,7] (▲), FBP-tBIA [4] (▼) and BPA-tBIA (◆).

substitution for the polymers of interest here. No clear trend was established for the O_2/N_2 solubility selectivity; as seen in Fig. 13(b), a slight increase for the PC polymers, a significant decrease for the HFBPA-tBIA polymers, and no significant change for the HFPC and BPA-tBIA polymers. The relatively small values of the O_2/N_2 solubility selectivity are sensitive to experimental error, which may partially explain the lack of clear trends. Similar plots for CO_2 solubility and CO_2/CH_4 solubility selectivity can be seen in Fig. 14(a) and (b). No clear trend can be established for the effect of bromine substitution on the CO_2 solubility selectivity; it decreases in the HFBPA-tBIA, PC and HFPC families and shows a mixed trend for the BPA-tBIA family. Likewise, there is no consistent trend for the CO_2/CH_4 solubility selectivity; the solubility selectivity decreases for the HFBPA-tBIA, PC and HFPC families and again exhibits a mixed trend for the BPA-tBIA family.

The changes in gas transport properties associated with bromine substitution for the five polymer families of interest were substantial. The oxygen permeability was reduced and the O_2/N_2 ideal selectivity increased significantly with bromine substitution; this combination of changes causes the bromine-substituted polymers to approach the Robeson 'upper bound'. The same trends were evident for CO_2/CH_4 permselectivity performance. The decreases in O_2 and CO_2 diffusivity and increases in O_2/N_2 and CO_2/CH_4 diffusivity selectivity were similar to those for permeability, and indicate that diffusivity contributions drive the gas transport changes associated with replacing methyl groups with bromine atoms. The small magnitude of the solubility selectivity changes indicates that polymer–penetrant interactions in bromine-substituted polymers are not the predominant reason for improved O_2/N_2 and CO_2/CH_4 selectivity.

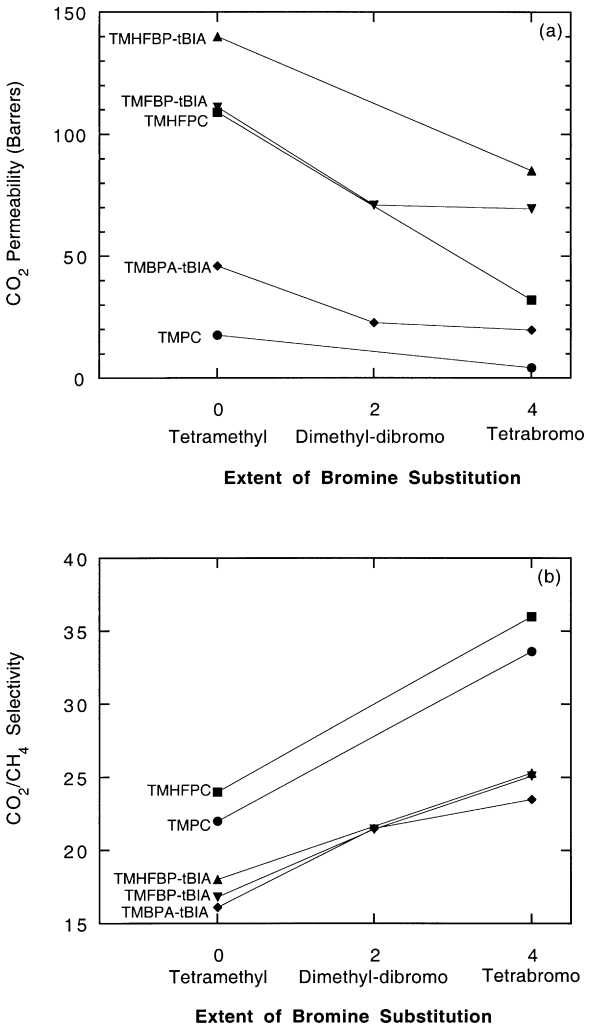

Fig. 10. Effect of replacing methyl groups with bromine atoms on (a) carbon dioxide permeability coefficients and (b) carbon dioxide/methane selectivity at 10 atm and 35°C for the families of substituted polymers studied: PC [3] (●), HFPC [2] (■), HFBP-tBIA [4,7] (▲), FBP-tBIA [4] (▼) and BPA-tBIA (◆).

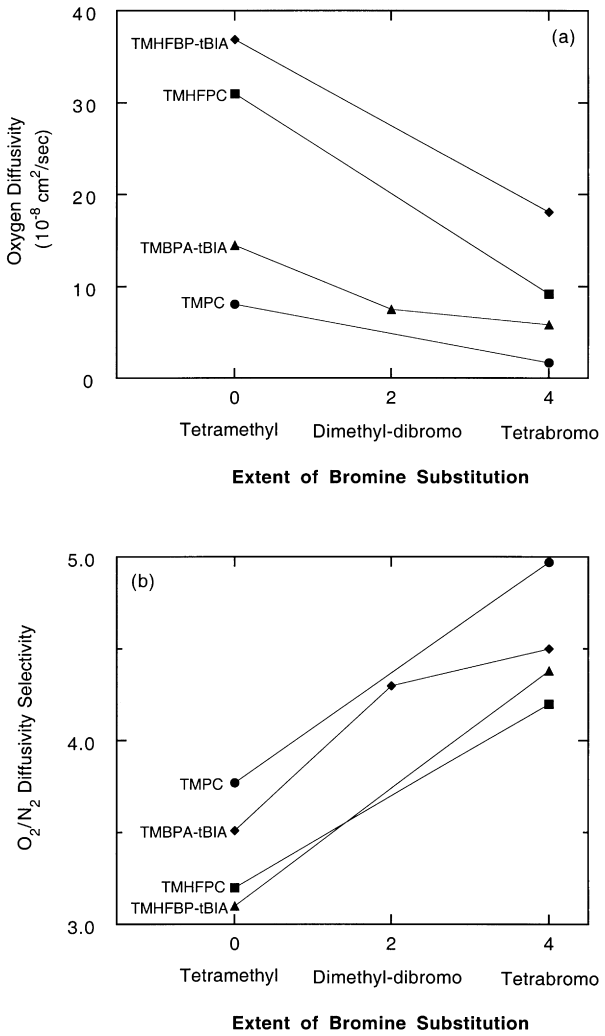

Fig. 11. Effect of replacing methyl groups with bromine atoms on (a) oxygen diffusion coefficients and (b) oxygen/nitrogen diffusivity selectivity at 2 atm and 35°C for the families of substituted polymers studied: PC [3] (●), HFPC [2] (■), HFBP-tBIA [4,7] (▲), FBP-tBIA [4] (▼) and BPA-tBIA (◆).

5.3. Effect of bromine substitution on energy parameters for substituted BPA-tBIA polymers

Fig. 15(a) shows that the permeation activation energy for N_2 is always larger than that for O_2 and both increase as the degree of bromine substitution increases; E_P increases with bromine substitution more strongly for N_2 than for O_2, as seen in Fig. 15(b). Similar plots for the CO_2/CH_4 pair are shown in Fig. 16. The curves are comparable to those seen for the O_2/N_2 pair. Both E_P (CO_2) and E_P (CH_4) increase as the degree of bromine substitution increases; as with the O_2/N_2 gas pair, E_P increases with bromine substitution more strongly for CH_4 than for CO_2, as seen in Fig. 16(b). The increase in the activation energies of permeation for all gases is consistent with the decrease in absolute permeability as methyl groups are replaced with bromine atoms, as seen in Fig. 9(a) and 10(a). Likewise, the increase in the difference in activation energies for permeation of N_2 relative to O_2 and of CH_4 relative to CO_2 is consistent with the increase in selectivity as bromine atoms replace methyl groups, as seen in Fig. 9(b) and 10(b).

Fig. 17 shows how the activation energies of diffusion for O_2 and N_2, and their difference, depend on bromine substitution. The activation energy of diffusion for nitrogen is larger than for oxygen in all three substituted polymers, and both activation energies of diffusion increase as bromine substitution increases. The difference in E_D for N_2 compared to O_2 increases significantly as bromine substitution increases. Similar plots for CO_2 and CH_4 can be seen in Fig. 18. The activation energy of diffusion for CH_4 is always greater than for CO_2 and both increase as

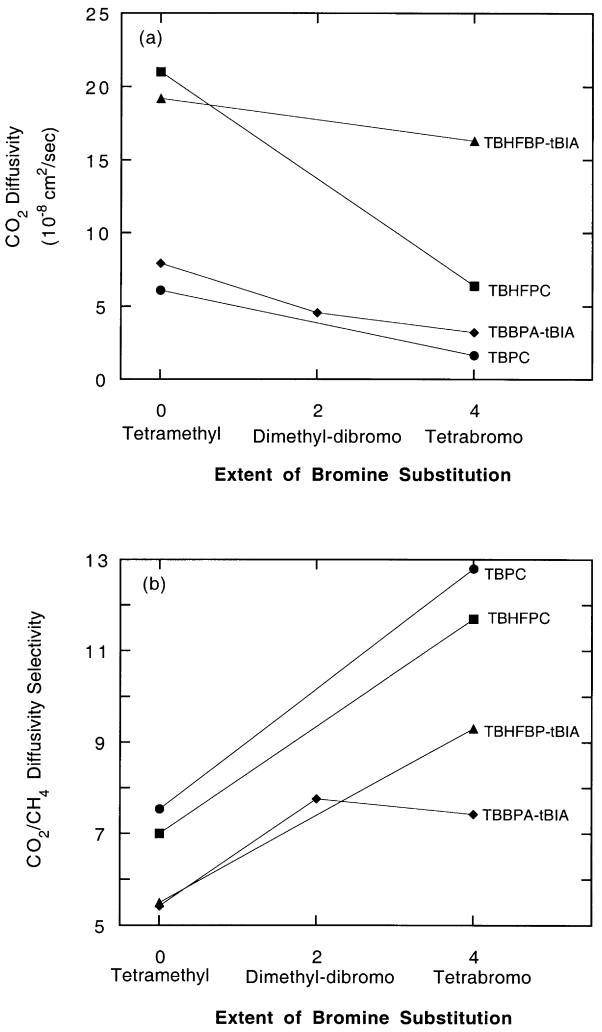

Fig. 12. Effect of replacing methyl groups with bromine atoms on (a) carbon dioxide diffusion coefficients and (b) carbon dioxide/methane diffusivity selectivity at 10 atm and 35°C for the families of substituted polymers studied: PC [3] (●), HFPC [2] (■), HFBP-tBIA [4,7] (▲), FBP-tBIA [4] (▼) and BPA-tBIA (♦).

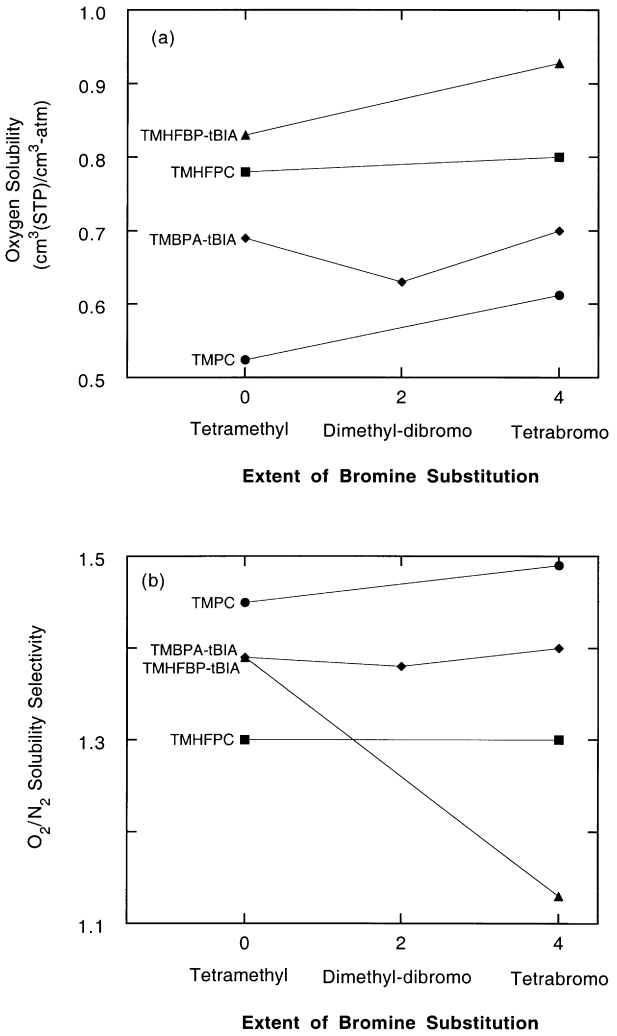

Fig. 13. Effect of replacing methyl groups with bromine atoms on (a) oxygen solubility coefficients and (b) oxygen/nitrogen solubility selectivity at 2 atm and 35°C for the families of substituted polymers studied: PC [3] (●), HFPC [2] (■), HFBP-tBIA [4,7] (▲), FBP-tBIA [4] (▼) and BPA-tBIA (♦).

bromine substitution increases; the curves are similar in magnitude but not in shape. As with permeation, the trend of increasing activation energies of diffusion and decreasing diffusivities (Fig. 11(a) and 12(a)) as bromine atoms are substituted for methyl groups is consistent. Moreover, the increase in O_2/N_2 and CO_2/CH_4 diffusivity selectivity as bromine atoms replace methyl groups (Fig. 11(b) and 12(b)) is consistent with the increase in the difference in activation energies for diffusion of N_2 relative to O_2 and of CH_4 relative to CO_2.

The differences in heat of sorption for penetrants are generally small compared to the analogous differences in activation energy of diffusion. The heats of sorption of O_2 and N_2 are plotted as a function of bromine substitution in Fig. 19. The values of H_S (N_2) and H_S (O_2) are rather similar for each polymer and generally tend to increase with bromine substitution; the trend is more consistent for N_2 than for O_2. The difference between the N_2 and O_2 values increases with bromine substitution (Fig. 19(b)). As seen in Fig. 20, the values of H_S (CH_4) and H_S (CO_2) decrease with increasing bromine substitution, and the difference is essentially constant (Fig. 20(b)).

The activation energies of diffusion for all gases increase with increasing bromine substitution; significant increases were seen in the E_D for N_2 relative to O_2 and for CH_4 relative to CO_2. Since E_D is a measure of the energy required for diffusional jumps of gas molecules through the polymer matrix, it is clear that bromine substitution makes the diffusion of N_2 less energetically favorable than that of O_2 and, similarly, CH_4 less favorable than CO_2. The changes in the activation energies for gas permeation in these polymers are dominated by changes in the activation energies of diffusion, and the heats of sorption play only a minor role.

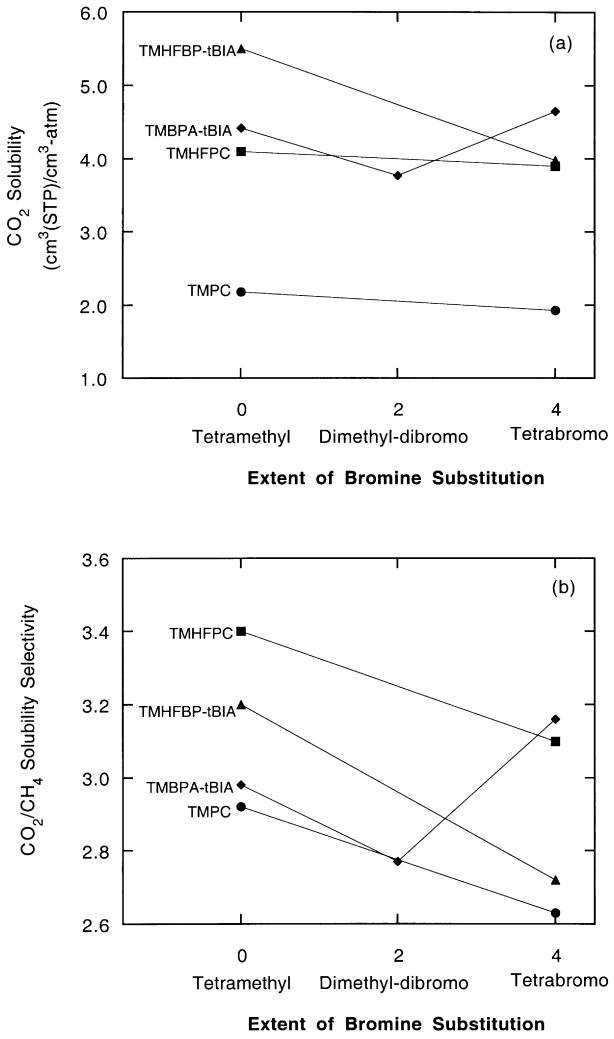

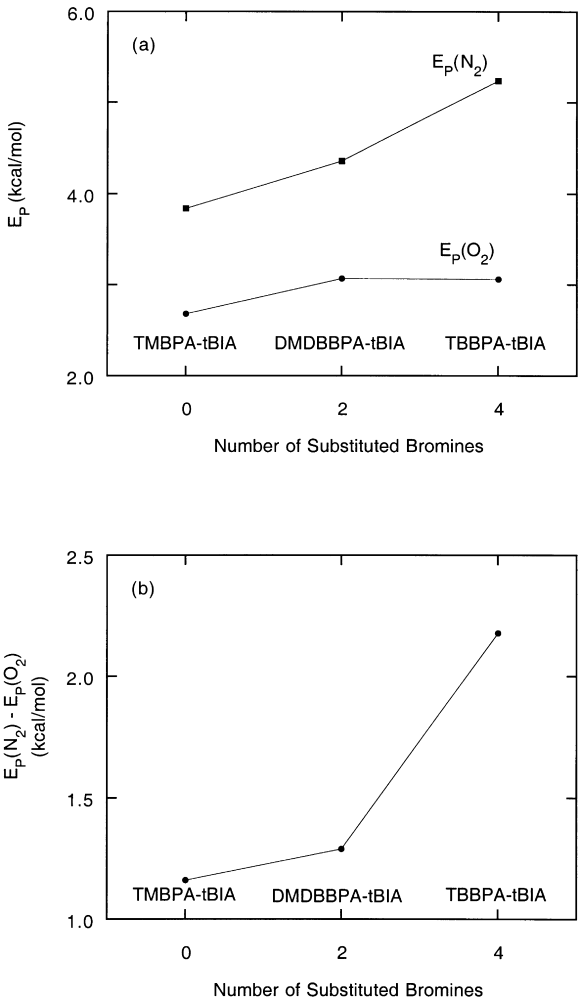

Fig. 14. Effect of replacing methyl groups with bromine atoms on (a) carbon dioxide solubility coefficients and (b) carbon dioxide/methane solubility selectivity at 10 atm and 35°C for the families of substituted polymers studied: PC [3] (●), HFPC [2] (■), HFBP-tBIA [4,7] (▲), FBP-tBIA [4] (▼) and BPA-tBIA (♦).

Fig. 15. The change in activation energies of permeation for oxygen and nitrogen (a) and their differences (b) as a function of degree of bromine substitution for the substituted BPA-tBIA polymer series.

6. Summary and conclusions

The effects of bromine substitution on physical and gas transport properties of five polymer families were investigated. Further, the response of one of these series of polymers, viz. substituted BPA-tBIA, to temperature was studied to establish how bromine substitution changes the activation energies of gas transport and to gain further insights about the O_2/N_2 and CO_2/CH_4 permselectivity response.

Bromine-substituted polymers exhibit high permeability and high selectivity which is desirable for membrane-based gas separation processes. High permeability is achieved due to the size of the bromine substituent, and improved O_2/N_2 selectivity is due to a more rigid and closely packed matrix; polar bromine atoms increase chain attraction and impede torsional rotation about the phenyl ring, as suggested by the higher cohesive energy density and glass transition temperature, respectively. These physical manifestations of bromine substitution affect the diffusion of oxygen and nitrogen through the polymer to different degrees. Compared to oxygen, the energy requirement for the diffusion of nitrogen through the brominated polymer is substantially higher. This gives rise to improved O_2/N_2 diffusivity selectivity and, thus, enhanced O_2/N_2 permselectivity for the bromine-substituted polymers. These same factors are responsible for the smaller but still significant improvement in CO_2/CH_4 permselectivity for the substituted BPA-tBIA polymers. The lack of change in O_2/N_2 solubility selectivity as a function of bromine substitution suggests that polymer/penetrant interactions do not contribute significantly to the overall permselectivity increase.

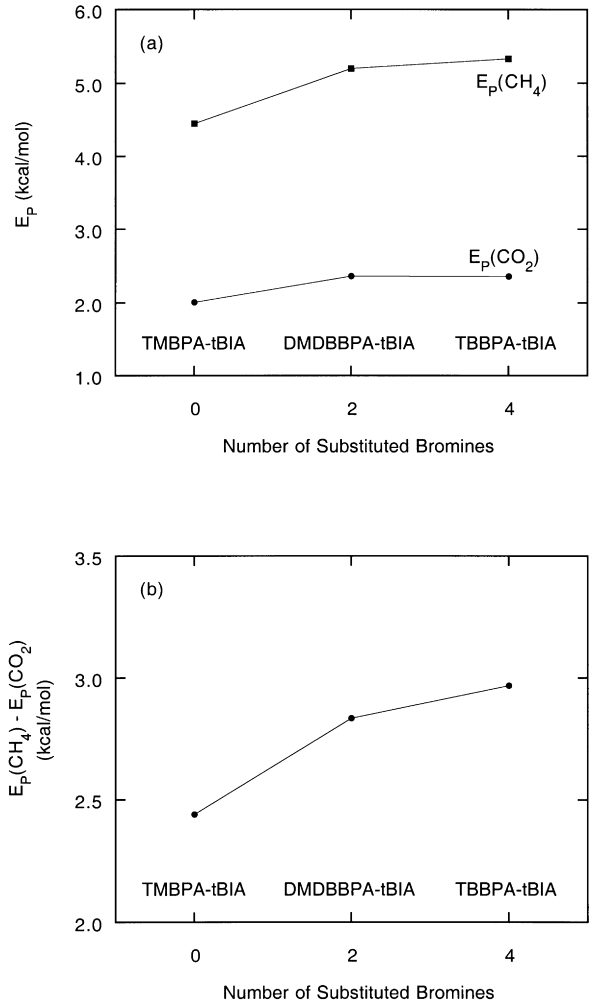

Fig. 16. The change in activation energies of permeation for carbon dioxide and methane (a) and their differences (b) as a function of degree of bromine substitution for the substituted BPA-tBIA polymer series.

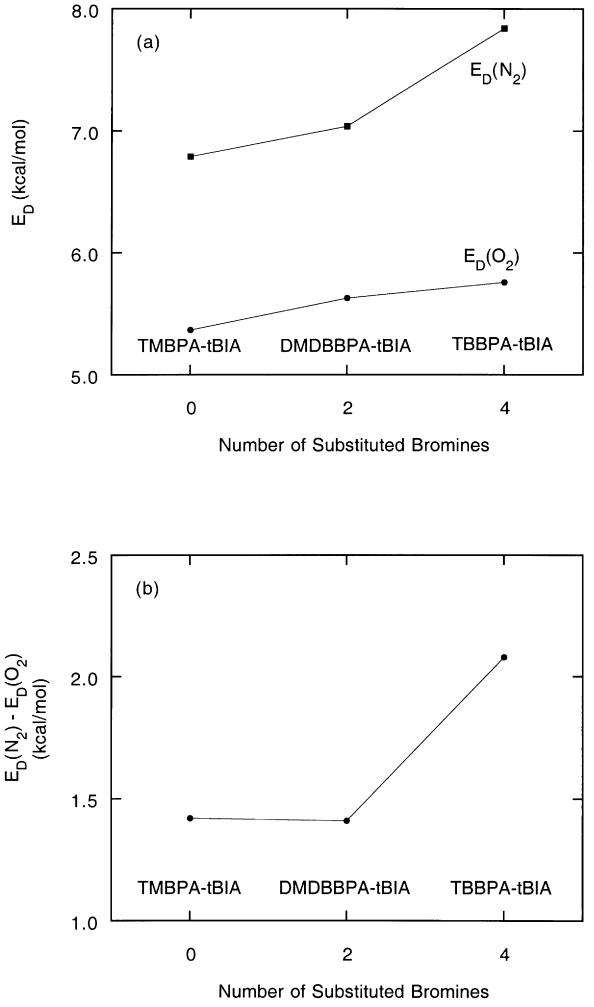

Fig. 17. The change in activation energies of diffusion for oxygen and nitrogen (a) and their differences (b) as a function of degree of bromine substitution for the substituted BPA-tBIA polymer series.

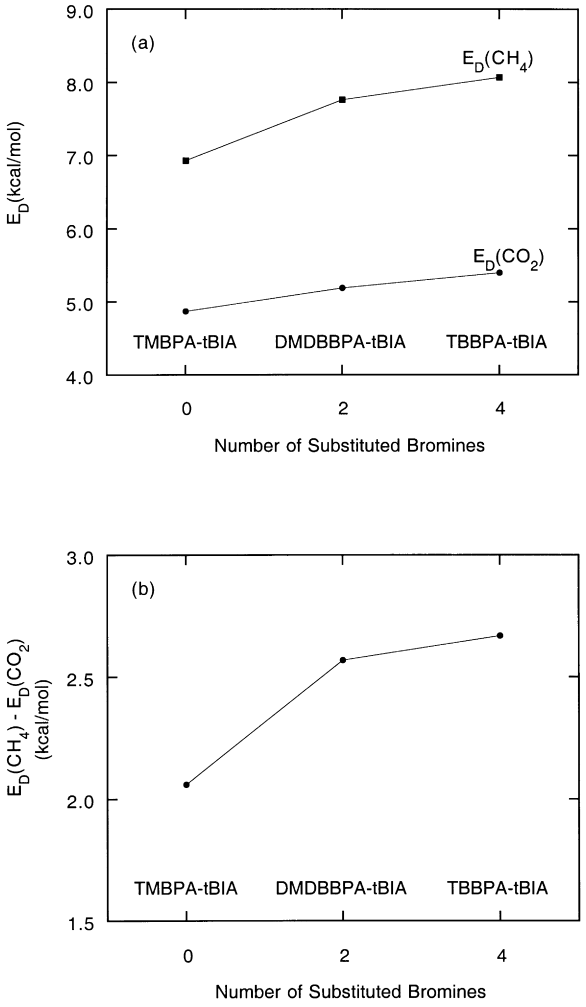

Fig. 18. The change in activation energies of diffusion for carbon dioxide and methane (a) and their differences (b) as a function of degree of bromine substitution for the substituted BPA-tBIA polymer series.

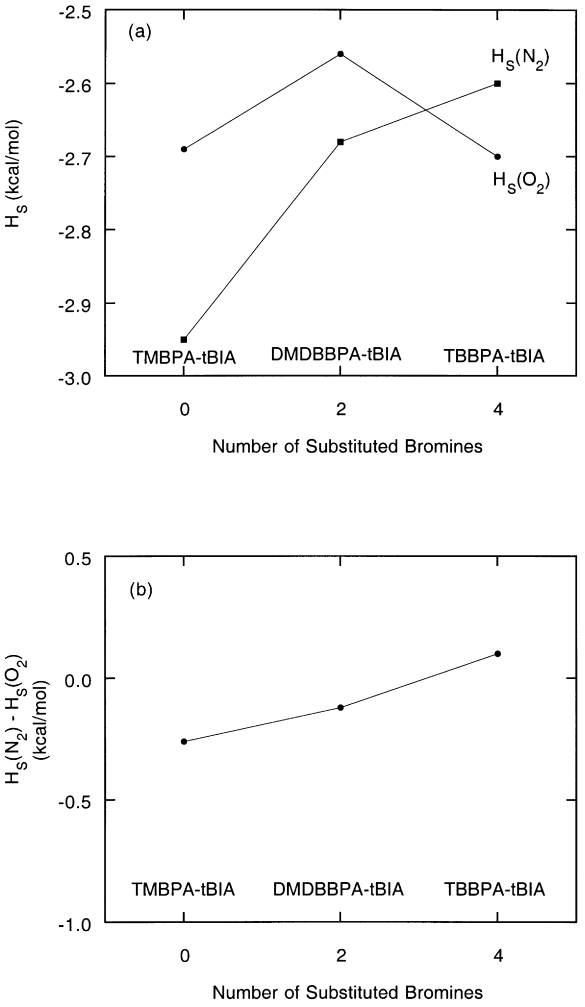

Fig. 19. The change in heats of gas sorption for oxygen and nitrogen (a) and their differences (b) as a function of degree of bromine substitution for the substituted BPA-tBIA polymer series.

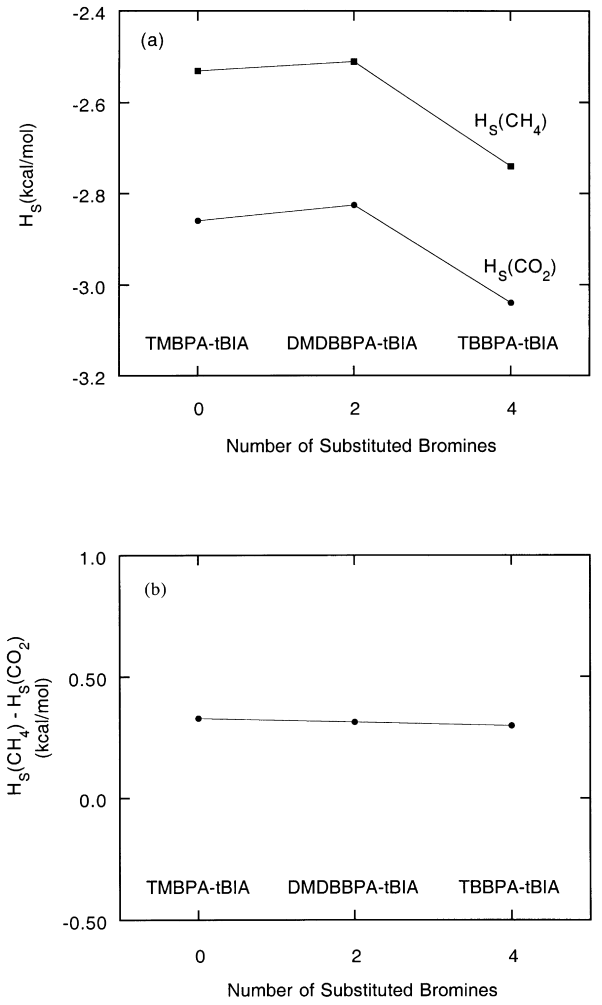

Fig. 20. The change in heats of gas sorption for carbon dioxide and methane (a) and their differences (b) as a function of degree of bromine substitution for the substituted BPA-tBIA polymer series.

Acknowledgements

This research was supported by the Separations Research Program at the University of Texas at Austin. Special thanks are extended to Amoco Chemical Company for supplying the 5-*t*-butyl isophthalic acid.

References

[1] Robeson LM. J Membr Sci 1991;62:165.
[2] Hellums MW, Koros WJ, Husk GR, Paul DR. J Appl Polym Sci 1991;43:1977.
[3] Muruganandam N, Koros WJ, Paul DR. J Polym Sci: Part B: Polym Phys 1987;25:1999.
[4] Pixton MR, Paul DR. J Polym Sci: Part B: Polym Phys 1995;33:1353.
[5] Pixton MR, Paul DR. J Polym Sci: Part B: Polym Phys 1995;33:1135.
[6] Hellums MW, Koros WJ, Husk GR, Paul DR. J Membr Sci 1989;46:93.
[7] Ruiz-Trevino A, Paul DR. J Appl Polym Sci 1998;68:403.
[8] Bondi A. Physical properties of molecular crystals, liquids and glasses. New York: John Wiley, 1968.
[9] Pixton MR, Paul DR. Macromolecules 1995;28:8277.
[10] Lo J, Lee SN, Pearce EM. J Appl Polym Sci 1984;29:35.
[11] Morgan PW. Macromolecules 1970;3:536.
[12] van Krevelen DW. Properties of polymers, 3rd ed. New York: Elsevier, 1990.
[13] Park JY, Paul DR. J Membr Sci 1997;125:23.